

Scaling theory of the Peierls charge density wave in metal nanowires

D. F. Urban,¹ C. A. Stafford,² and Hermann Grabert¹

¹Physikalisches Institut, Albert-Ludwigs-Universität, D-79104 Freiburg, Germany

²Department of Physics, University of Arizona, Tucson, Arizona 85721, USA

(Received 8 November 2006; revised manuscript received 30 January 2007; published 17 May 2007)

The Peierls instability in multichannel metal nanowires is investigated. Hyperscaling relations are established for the finite-size, temperature, and wave-vector scaling of the electronic free energy. It is shown that the softening of surface modes at wave vector $q=2k_{F,\nu}$ leads to critical fluctuations of the wire's radius at zero temperature, where $k_{F,\nu}$ is the Fermi wave vector of the highest occupied channel. This Peierls charge density wave emerges as the system size becomes comparable to the channel correlation length. Although the Peierls instability is weak in metal nanowires, in the sense that the correlation length is exponentially long, we predict that nanowires fabricated by current techniques can be driven into the charge-density-wave regime under strain.

DOI: [10.1103/PhysRevB.75.205428](https://doi.org/10.1103/PhysRevB.75.205428)

PACS number(s): 73.21.Hb, 68.65.La, 71.45.Lr, 72.15.Nj

I. INTRODUCTION

Already long ago, Fröhlich¹ and Peierls² pointed out that a one-dimensional metal coupled to the underlying lattice is not stable at low temperatures. Electron-phonon interactions lead to a novel type of ground state with a charge density wave (CDW) of wave vector $2k_F$ (see Ref. 3 for a review). This state is characterized by a gap in the single-particle excitation spectrum, and by a collective mode with an associated charge density $\sim \rho_0 + \rho_1 \cos(2k_F z)$, where ρ_0 is the unperturbed electron density of the metal. Of particular interest are *incommensurate* systems, where the period of the CDW is not simply related to that of the unperturbed atomic structure. In that case, no long-range order is expected even at zero temperature due to quantum fluctuations.

In contrast to the usual Peierls systems, metallic nanowires⁴ are open systems with several inequivalent channels, for which the theory has not yet been developed. Interest in the Peierls transition in metal nanowires has been stimulated by recent experiments⁵⁻⁹ on nanowire arrays on stepped surfaces. In these systems, interactions between nanowires, mediated by the substrate, render the system quasi-two-dimensional at low temperatures, similar to the dimensional crossovers commonly observed in highly anisotropic organic conductors.³ However, individual freestanding metal nanowires⁴ represent true (quasi-)one-dimensional systems, in which the intrinsic behavior of the Peierls CDW can be studied.

Due to quantization perpendicular to the wire axis, electron states in metal nanowires are divided into distinct channels, which are only weakly coupled. Each channel has a quadratic dispersion relation, and starts to contribute at a certain threshold energy, i.e., the eigenenergy E_n of the corresponding transverse mode. This results in a sequence of quasi-one-dimensional systems with different Fermi wave vectors,

$$k_{F,n} = \sqrt{\frac{2m_e}{\hbar^2}(E_F - E_n)}. \quad (1)$$

The channel Fermi wave vectors are generically *not com-*

mensurate with the underlying atomic structure in nanowires with more than one open channel.

The Peierls instability is weak in metal nanowires,¹⁰ so that the system is close to the quantum critical point at which the transition from Fermi-liquid behavior to a CDW state occurs. In the vicinity of the quantum critical point, the system exhibits an additional length scale, the correlation length

$$\xi_\nu = \frac{\hbar v_{F,\nu}}{2\Delta_\nu}. \quad (2)$$

Here, the greek index ν labels the highest occupied channel, in which an energy gap $2\Delta_\nu$ opens, and $v_{F,\nu} = (\hbar/m_e)k_{F,\nu}$ is the Fermi velocity of this subband. Within a hyperscaling ansatz,¹¹ the singular part of the energy is expected to scale like $E_{\text{sing}}/L \sim \xi_\nu^{-1-z}$, where L is the wire length, and the dynamic critical exponent takes the value $z=1$. Thus, $E_{\text{sing}}/L \sim \Delta_\nu^2/\hbar v_{F,\nu}$. Near the singular point, we indeed find that the electronic energy is given by

$$\frac{E_{\text{sing}}}{L} \approx \kappa_\nu \frac{\Delta_\nu^2}{\hbar v_{F,\nu}} Y\left(\xi_\nu \delta q, \frac{\xi_\nu}{L}, \frac{\xi_\nu}{L_T}\right), \quad (3)$$

where $Y(x,y,z) \approx \ln(\max\{x,y,z\})$ is a universal and dimensionless scaling function, $\delta q = (q - 2k_{F,\nu})$ is the detuning of the perturbation wave vector from its critical value $2k_{F,\nu}$, $L_T = \hbar v_{F,\nu}/k_B T$ is the thermal length at temperature T , and $\kappa_\nu = 1$ or 2 is the degeneracy of the highest open channel ν . This universal scaling behavior is quite different from that of a closed system with periodic boundary conditions,^{12,13} where radically different behavior was found for odd or even numbers of fermions. Nonetheless, the correlation length ξ was also found to control the finite-size scaling of the Peierls transition in mesoscopic rings.¹³

In this paper, the quantum and thermal fluctuations of the nanowire surface are calculated in a continuum model,¹⁴ where the ionic background is treated as an incompressible, irrotational fluid. In contrast to the semiclassical theory of Ref. 14, which exhibited critical surface fluctuations only at finite temperature (due to the classical Rayleigh instability), the present fully quantum-mechanical theory exhibits critical zero-temperature surface fluctuations at wave vector q

$=2k_{F,\nu}$. In a finite system, these CDW correlations are found to grow in amplitude as the wire length L approaches a critical length L_c of the order of the correlation length ξ_ν . A similar scaling is observed as the temperature is lowered, so that L_T exceeds ξ_ν . Although ξ_ν is typically very large for fully equilibrated structures, consistent with the fact that Peierls distortions have not yet been observed in multichannel nanowires, it is predicted that nanowires of dimensions currently produced in the laboratory can be driven into the CDW regime by applying strain.

This paper is organized as follows. Section II summarizes the (standard) Peierls theory for a one-dimensional metal with a half-filled band, and extends it to multichannel wires. A description of the deformation of a nanowire through surface phonons is given in Sec. III. The correlation length ξ is introduced in Sec. IV, and the scaling relation (3) is established. Section V examines the critical surface fluctuations, and consequences for different materials are discussed. Finally, a summary and discussion are given in Sec. VI.

II. PEIERLS INSTABILITY

Consider the ground state of a one-dimensional linear chain of atoms, with lattice constant a and periodic boundary conditions. In the presence of electron-phonon interactions, it is energetically favorable to introduce a periodic lattice distortion with period $\lambda = \pi/k_F$; this effect is known as the Peierls instability.² The lattice distortion opens up an energy gap 2Δ in the electronic dispersion relation at the Fermi level E_F , so that the total electronic energy is lowered. If $\Delta \ll E_F$, then the gain in energy is given by²

$$\frac{E_{\text{gain}}}{L} \approx \frac{1}{\pi} \frac{\Delta^2}{2E_F/k_F} \left[\log\left(\frac{\Delta}{4E_F}\right) - \frac{1}{2} \right] + \mathcal{O}\left(\frac{\Delta}{E_F}\right)^4. \quad (4)$$

The size of the gap can be extracted from an energy balance: Let the increase of the elastic energy due to the deformation be given by $E_{\text{cost}}/L = \alpha b^2$, where b is the amplitude of the distortion. On the other hand, Δ is defined through the matrix element of the perturbation coupling states with longitudinal wave vector $\pm k_F$; it is linear in b and we can set $\Delta = Ab$. By finding the minimum of $\delta E(b) = E_{\text{gain}} + E_{\text{cost}}$, we can derive the optimal value of the distortion amplitude b and from this derive the size Δ of the gap,

$$\Delta = 4E_F \exp(-2\pi\alpha E_F/A^2 k_F). \quad (5)$$

The analysis of the Peierls instability in a one-dimensional metal can be extended to the case of a multichannel system. While other instabilities of the Fermi liquid—induced by electron-electron interactions—compete with the Peierls instability in purely one-dimensional systems,³ their importance decreases as the number of channels increases,¹⁵ so that electron-electron interactions can, in a first approximation, be neglected in multichannel nanowires. Moreover, electron-electron interactions are strongly screened in s -orbital metal nanowires with three or more conducting channels.^{16,17} Hence, including electron-electron interactions in the calculation will not lead to any qualitative change (except in the limit of very few conduction channels),

whereas electron-phonon interactions do.¹⁸ We therefore consider only electron-phonon coupling in this paper.

For any given channel n , a perturbation of wave vector $q = 2k_{F,n}$ will open a gap $2\Delta_n$ at the Fermi surface in the energy dispersion of this channel. The energy gain $E_{\text{gain},n}$ and gap size $2\Delta_n$ are then given by Eqs. (4) and (5), respectively, with k_F replaced by $k_{F,n}$ and E_F replaced by $\hbar^2 k_{F,n}^2 / 2m_e$. The greatest effect will be seen close to the opening of the highest occupied channel (i.e., $n = \nu$), where the channel Fermi wave vector $k_{F,\nu}$ is small. Note that the same perturbation (with $q = 2k_{F,\nu}$) will also modify the dispersion relations of lower-energy channels n' with $E_{n'} < E_\nu$, but due to the finite spacing of the threshold energies, this modification will occur within the Fermi sea and there will be little net effect.¹⁰

The standard Peierls theory uses periodic boundary conditions for the wave functions. Its extension to the multichannel case cannot be directly applied to a metallic nanowire of finite length L . The nanowire is part of a much larger system including the leads, and the longitudinal wave vectors k_n in the subbands are not restricted to multiples of $\frac{2\pi}{L}$, as in the case of an isolated system with periodic boundary conditions. Therefore, a perturbation of the nanowire with wave vector q does not only couple states k_n and k'_n that exactly obey $k_n = k'_n + q$. Instead, the state k_n is coupled to a range of k'_n states proportional to $1/L$. The dispersion relation remains smooth while, with increasing wire length, it develops a smeared-out *quasigap*, and only in the limit $L \rightarrow \infty$ do we recover the Peierls result with a jump at $k_{F,n}$.¹⁰

III. SURFACE PHONONS

We describe the wire in terms of the nanoscale free-electron model (NFEM),^{19,20} treating the electrons as a Fermi gas confined within the wire by a hard-wall potential. The ionic structure is replaced by a uniform (jellium) background of positive charge, and we assume that this ionic medium is irrotational and incompressible. The approximations^{14,16,20} of the NFEM require strong delocalization of the valence electrons, good charge screening, and a spherical Fermi surface, conditions met in alkali metals and, to a lesser extent, noble metals such as gold.

In this continuum model, the ionic degrees of freedom are completely determined by the surface coordinates of the wire. Let us consider an initially uniform wire of radius R_0 and length L which is axisymmetrically distorted. Its surface is given by the radius function

$$R(z, t) = R_0 \left(1 + \sum_q b_q(t) e^{iqz} \right), \quad (6)$$

where the time-dependent perturbation is written as a Fourier series with coefficients $b_q(t)$. Since $R(z, t)$ is real, we have $b_q = b_{-q}^*$ and we require that the volume of the wire is unchanged by the deformation. Other physically reasonable constraints are possible and will be discussed in detail in Sec. V.

The kinetic energy of the ionic medium is given by¹⁴

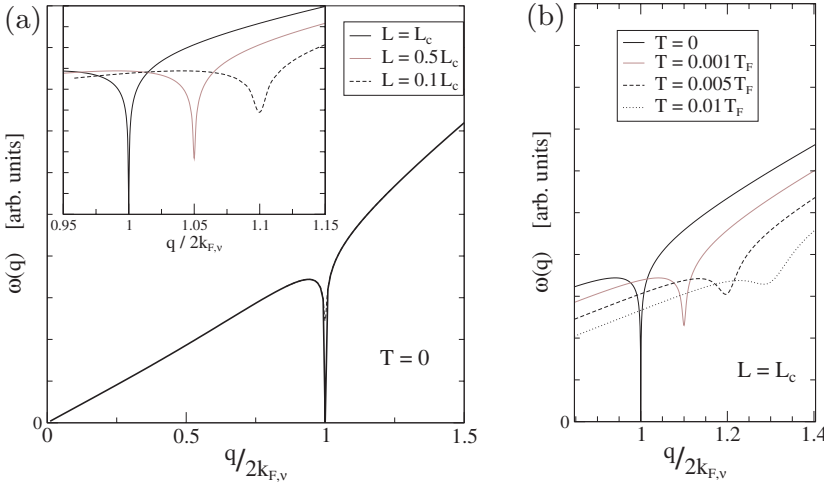


FIG. 1. (Color online) (a) Surface phonon dispersion relation $\omega(q)$ for a wire of length $L=L_c$, where L_c is the critical length (see text). Different wire lengths are compared in the inset showing the vicinity of $q=2k_{F,\nu}$. The curves are offset horizontally by 0.05 units for clarity. (b) Temperature dependence of the minimum in $\omega(q)$ for a wire of length $L=L_c$ (curves are offset horizontally by 0.1 units). The wire radius is $R_0=4.5k_F^{-1}$ for all curves, thus $L_c \sim 6500k_F^{-1}$.

$$E_{kin} = L \sum_{q>0} m(q, R_0) \left| R_0 \frac{\partial b_q(t)}{\partial t} \right|^2. \quad (7)$$

Here, the *mode inertia* m is a function of wire radius and phonon wave vector and reads

$$m(q, R_0) = \rho_{ion} \frac{2\pi R_0 I_0(qR_0)}{q I_1(qR_0)}, \quad (8)$$

where ρ_{ion} is the ionic mass density, and I_0 and I_1 are the modified Bessel functions of zeroth and first order, respectively.²¹ Considered as a function of q , the mode inertia has a singularity $\sim 1/q^2$ at $q=0$ and is monotonically decreasing, with $m \sim 1/q$ for large q .

Within the Born-Oppenheimer approximation, the potential energy of the ions is given by the grand canonical potential Ω of the confined electron gas. A linear stability analysis of cylindrical wires determining the leading-order change in Ω due to a small perturbation was recently presented in Ref. 10: $\delta\Omega$ is quadratic in the Fourier coefficients b_q of the deformation, and can be written as

$$\frac{\delta\Omega}{L} = \sum_{q \geq 0} |b_q|^2 \alpha(q, R_0, L, T) + \mathcal{O}\left(\frac{\lambda_F}{L}\right), \quad (9)$$

where the terms of order λ_F/L include nondiagonal contributions which can be neglected if the wire is long enough.²² The explicit analytical expression for the *mode stiffness* α is given in Appendix A. Here, we are interested in the general behavior of the mode stiffness as a function of the perturbation wave vector q for a given radius R_0 , length L , and temperature T : $\alpha(q)$ is a smoothly increasing function, with a L - and T -dependent dip at $q=2k_{F,\nu}$, where ν is the index of the highest open channel (see Appendix A). Therefore, we formally split α into a smoothly varying term and one containing the singular contribution of channel ν ,

$$\alpha = \alpha_{smooth} + \alpha_{sing}^{(\nu)}. \quad (10)$$

The smooth part can be thought of as the sum of a Weyl contribution,¹⁴ which describes the effects of surface tension σ_s and curvature energy γ_s , plus an electron-shell correction,¹⁴

$$\alpha_{smooth} = -2\pi R_0 \sigma_s + 2\pi R_0^2 (\sigma_s R_0 - \gamma_s) q^2 + \alpha_{shell}, \quad (11)$$

whereas the singular part describes the onset of the Peierls instability in channel ν . At zero temperature, it is given by¹⁰

$$\alpha_{sing}^{(\nu)}(q, R_0, L) = -\frac{2m_e}{\hbar^2} \frac{4\kappa_\nu E_\nu^2}{\pi q} \left[\ln \left| \frac{2k_{F,\nu} + q}{2k_{F,\nu} - q} \right| - F((2k_{F,\nu} + q)L) + F(|2k_{F,\nu} - q|L) \right], \quad (12)$$

where $F(x) = \text{Ci}(x) - \sin(x)/x$ and $\text{Ci}(x)$ is the cosine integral function.²³ The finite-temperature mode stiffness is evaluated numerically by computing the integral

$$\alpha(T) = \int dE \left(-\frac{\partial f}{\partial E} \right) \alpha(E), \quad (13)$$

where $f(E)$ is the Fermi function and $\alpha(E)$ is obtained from the zero-temperature results by replacing $k_{F,\nu}$ by $k_{E,\nu} \equiv \left[\frac{2m_e}{\hbar^2} (E - E_\nu) \right]^{-1/2}$.

Combining the kinetic energy (7) and potential energy (9) yields a Hamiltonian for surface phonons, $H_{ph} = \sum_q \hbar \omega_q (\hat{a}_q^\dagger \hat{a}_q + \frac{1}{2})$, with frequencies

$$\omega(q, R_0, L, T) = \sqrt{\frac{\alpha(q, R_0, L, T)}{R_0^2 m(q, R_0)}}. \quad (14)$$

These axisymmetric surface phonons correspond to the longitudinal-acoustic mode of the nanowire. From Eqs. (8), (10), and (14), we infer that $\omega(q)$ is a smoothly increasing function of q , with a dip at $q=2k_{F,\nu}$. As expected for acoustic phonons, it is linear for small q . The L -dependent softening of the phonon modes with wave vector $2k_{F,\nu}$ defines a *critical length* L_c for which $\omega(2k_{F,\nu})=0$.

A plot of $\omega(q)$ for $L=L_c$ at zero temperature is shown in Fig. 1(a). The inset shows a close-up of the minimum and compares different wire lengths, where the curves are horizontally offset for clarity. The temperature dependence of ω is illustrated in Fig. 1(b), concentrating on the vicinity of q

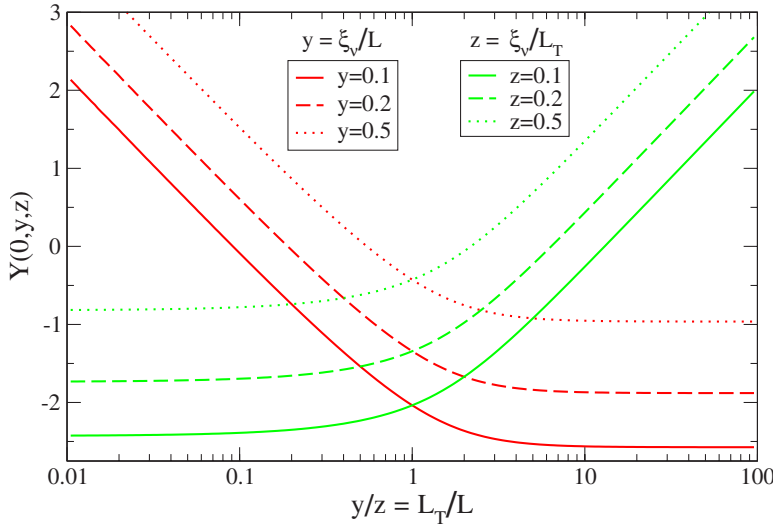


FIG. 2. (Color online) Crossover from T scaling to L scaling: The scaling function $Y(x, y, z)$ is plotted as a function of the ratio $y/z = L_T/L$ for fixed values of $y = \xi_v/L$ (red curves) and $z = \xi_v/L_T$ (green curves) at $x = \delta q \xi_v = 0$. For all curves, $R_0 = 8k_F^{-1}$.

$= 2k_{F,\nu}$ (again, the curves are horizontally offset). With increasing temperature, the dip in ω disappears, and the curve becomes smoother.

IV. SCALING RELATIONS

The opening of the Peierls gap in subband ν introduces a new energy scale, given by the gap $2\Delta_\nu$ for an infinitely long wire. Δ_ν is determined by the matrix element of the perturbation coupling states with longitudinal wave vector $\pm k_{F,\nu}$ and is linear in the distortion amplitude b_q . The perturbation potential matrix element is calculated in Appendix B, and we find that $\Delta_\nu = 2E_\nu b_q$.

On the other hand, the energy cost for creating a surface modulation with wave vector q is determined by the smooth part of the mode stiffness, so that $\delta E_{\text{cost}}/L = \alpha_{\text{smooth}}(q)|b_q|^2$. Following the arguments of Sec. II, we can now calculate the length scale ξ_ν , obtaining

$$\xi_\nu = \frac{\hbar v_{F,\nu}}{2\Delta_\nu} = \frac{1}{4k_{F,\nu}} \exp \left[\left(\frac{\hbar^2}{2m_e} \right) \frac{\pi k_{F,\nu} \alpha_{\text{smooth}}}{2\kappa_\nu E_\nu^2} \right], \quad (15)$$

where we have used Eq. (5). Introducing the correlation length ξ_ν allows us to derive the finite-size, temperature, and wave-vector scaling of the electronic free energy near the critical point of the Peierls instability, given by $q = 2k_{F,\nu}$, $L \rightarrow \infty$, $T = 0$, and weak electron-phonon coupling.

Finite-size scaling. First, we examine the mode stiffness at zero temperature and for $q = 2k_{F,\nu}$ as a function of wire length. Starting from Eqs. (10) and (12), we take the limit $q \rightarrow 2k_{F,\nu}$ and get

$$\alpha(L)|_{q=2k_{F,\nu}} = \alpha_{\text{smooth}} - \frac{4\kappa_\nu E_\nu^2}{\pi \hbar v_{F,\nu}} [\ln(4k_{F,\nu}L) - c_1], \quad (16)$$

where $c_1 = 1 - \gamma_E + F(4k_{F,\nu}L) \approx 0.42$. Here, $\gamma_E \approx 0.577$ is the Euler-Mascheroni constant, and we have used the fact that $F(x) \ll 1$ for $x \gg 1$. This expression for $\alpha(L)$ can further be simplified by the use of Eq. (15), so that

$$\alpha(L)|_{q=2k_{F,\nu}} = \frac{4\kappa_\nu E_\nu^2}{\pi \hbar v_{F,\nu}} \left[\ln \left(\frac{\xi_\nu}{L} \right) + c_1 \right]. \quad (17)$$

This defines the critical length L_c for which α takes the value zero,

$$L_c \equiv e^{c_1} \xi_\nu \approx 1.52 \xi_\nu. \quad (18)$$

Note that the critical length is of the same order of magnitude as the correlation length.

Wave-vector scaling. Now let $\delta q \equiv (q - 2k_{F,\nu})$ be the detuning of the perturbation wave vector from its critical value $2k_{F,\nu}$. At zero temperature and in the limit $L \rightarrow \infty$, we expand the mode stiffness as a function of δq and obtain

$$\alpha(\delta q)|_{L=L_c} = \frac{4\kappa_\nu E_\nu^2}{\pi \hbar v_{F,\nu}} \ln |\xi_\nu \delta q| + \mathcal{O}(\delta q). \quad (19)$$

Again, the result was written in a compact form by the use of Eq. (15).

Temperature scaling. Finally, we examine the effect of finite temperature for a wire of infinite length and a perturbation of wave vector $2k_{F,\nu}$. The main effect of finite temperature is to smear out the Fermi surface, so that the critical wave vector q is detuned by $\delta q_E = 2(k_{F,\nu} - k_{E,\nu})$ with $k_{E,\nu} \equiv \left[\frac{2m_e}{\hbar^2} (E - E_\nu) \right]^{-1/2}$. Starting from the scaling behavior for finite δq detuning [Eq. (19)], we calculate $\alpha(T)$ for small T from Eq. (13) by linearizing $E - E_F \approx \hbar v_{F,\nu} (k_{E,\nu} - k_{F,\nu})$ and find

$$\alpha(T)|_{q=2k_{F,\nu}} = \frac{4\kappa_\nu E_\nu^2}{\pi \hbar v_{F,\nu}} \left[\ln \left| \frac{\xi_\nu}{\hbar v_{F,\nu} \beta} \right| + c_2 \right], \quad (20)$$

with a numerical constant $c_2 = -\gamma_E + \ln \pi \approx 0.57$.

Combining the three scaling relations for length, perturbation wave vector, and temperature, Eqs. (17), (19), and (20), respectively, we prove Eq. (3) for the singular part of the electronic energy.²⁴

Finite temperature introduces a thermal length $L_T = \beta \hbar v_{F,\nu}$. Changing L_T has an equivalent influence on the system properties as changing the length of the wire L . Near the critical point, we observe a crossover between finite- T

scaling and finite- L scaling, depending on the ratio L_T/L (see Fig. 2). The smaller of the two lengths dominates the behavior of the singular part of the electronic energy. As long as $L_T < L$, a change of L , even by orders of magnitude, has only a small effect on Y , whereas the system is sensitive to small changes in L_T and shows T scaling. The situation is reversed for $L_T > L$: In this case, a change in temperature results in only small changes of Y , whereas the singular part of the energy depends strongly on L and shows finite-length scaling. These two different cases are illustrated in Fig. 2 by the two sets of curves for different fixed values of L and L_T , respectively.

So far, we have considered ideal nanowires without disorder. Disordered structures exhibit an additional length scale, the electron elastic mean free path ℓ . The scaling theory we have derived allows us to predict that the effect of disorder is to cut off the logarithmic scaling of the Peierls CDW instability, exactly like the thermal length or wire length. We thus infer that the length-dependent criterion for the emergence of the Peierls CDW in metal nanowires is given by

$$L_c \leq L, L_T, \ell, \quad (21)$$

where the critical length L_c [Eq. (18)] is of the order of the correlation length ξ_ν . Increasing temperature leads to a decreasing thermal length, and therefore destroys the phenomenon at sufficiently high T . Increasing disorder has a corresponding effect.

V. SURFACE FLUCTUATIONS

The softening of the surface phonon modes with wave vector $q=2k_{F,\nu}$ leads to critical surface fluctuations. Given the mode stiffness α and phonon frequency $\omega(q)$, the fluctuations about the cylindrical shape are given by²⁵

$$\frac{\langle R(z)R(0) \rangle}{R_0^2} = \frac{1}{2\pi} \int_{-\infty}^{\infty} dq \frac{\hbar \omega(q)}{\alpha(q)} \left[\frac{1}{e^{\beta \hbar \omega(q)} - 1} + \frac{1}{2} \right] e^{iqz}. \quad (22)$$

Figure 3 shows the correlations for different wire lengths at zero temperature. Fluctuations with $q=2k_{F,\nu}$ increase with increasing wire length. Note that these CDW correlations may be pinned by disorder, or at the wire ends.³ The correlations shown in Fig. 3 are representative of regions far from an impurity or wire end.

For large z , we can use a saddle-point approximation to estimate the integral in Eq. (22), and find

$$\frac{\langle R(z)R(0) \rangle}{R_0^2} \propto \cos(2k_{F,\nu} z) K_0 \left(\sqrt{12 \log(L_c/L)} \frac{z}{L} \right), \quad (23)$$

where K_0 is the modified Bessel function of the second kind²⁶ of order 0. Its asymptotic behavior is given by²⁷

$$K_0(x) \sim \begin{cases} -\gamma_E - \log x/2 & \text{for } x \ll 1 \\ \sqrt{\frac{\pi}{2x}} e^{-x} & \text{for } x \gg 1. \end{cases} \quad (24)$$

Depending on the ratio of the wire length L to the critical length L_c , we can distinguish two regimes: for $L \leq L_c$, the

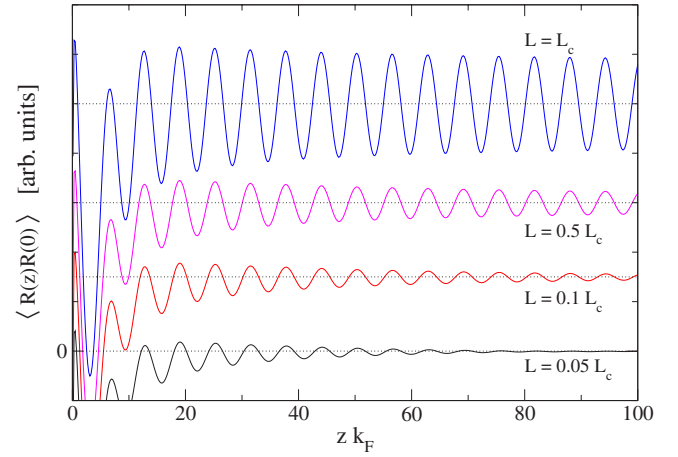


FIG. 3. (Color online) CDW correlations for various values of L/L_c at $T=0$ for a wire with $R=4.42k_F^{-1}$. The critical length is $L_c \sim 1560k_F^{-1}$. Curves offset vertically for clarity.

prefactor of z/L in the argument of K_0 in Eq. (23) is large and the correlations decay exponentially for sufficiently large z . On the other hand, if $L \sim L_c$, our theory predicts a logarithmic decay of the correlations. Note that the ratio L/L_c determines the crossover from a regime where the harmonic approximation about a Fermi liquid is valid ($L < L_c$) to that of a fully developed CDW ($L > L_c$). The harmonic approximation, which we have used in our calculation, breaks down at $L=L_c$, where the wire can no longer be treated as a cylinder with small perturbations.

The correlation length ξ is a material-specific quantity, since it depends exponentially on the smooth contribution (11) to the mode stiffness [see Eq. (15)]. As discussed in detail in Ref. 28, the material-specific surface tension and curvature energy can be included in the NFEM through a generalized constraint on the allowed deformations of the wire,

$$\mathcal{N} = k_F^3 \mathcal{V} - \eta_s k_F^2 \mathcal{S} + \eta_c k_F \mathcal{C} = \text{const.} \quad (25)$$

Here, \mathcal{V} is the volume of the wire, \mathcal{S} its surface area, and \mathcal{C} its integrated mean curvature. The constraint $\partial \mathcal{N} = 0$ restricts the number of independent Fourier coefficients in Eq. (6), and allows b_0 to be expressed in terms of the other Fourier coefficients. This results in a modification of the smooth part of the mode stiffness (see Appendix A). Through an appropriate choice of the dimensionless parameters η_s and η_c , the surface tension and curvature energy can thus be set to the appropriate values for any given material.²⁸

The upper panel of Fig. 4 shows the correlation length calculated using the material parameters²⁹ for Na and Au. For clarity, the plot is restricted to the cylindrical wires of so-called *magic radii* that prove to be remarkably stable even when allowing symmetry-breaking deformations.^{28,30} These wires have conductance values $G/G_0 = 1, 3, 6, 12, 17, 23, 34, 42, 51, \dots$, where $G_0 = 2e^2/h$ is the conductance quantum.³¹ Arrows point to the positions of the most stable wires, defined as those with the longest estimated lifetimes,³² which are near the minima of the shell potential for straight cylindrical wires, shown in the lower panel of Fig. 4.

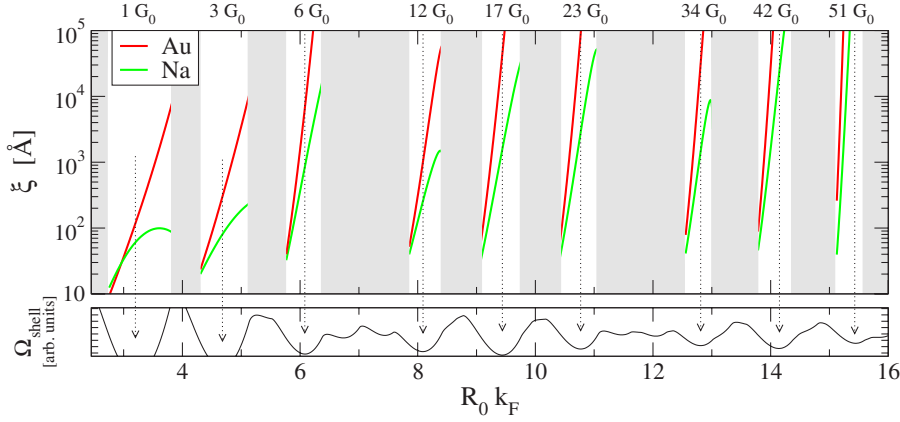


FIG. 4. (Color online) Upper panel: Correlation length ξ_v for Na and Au. For clarity, the plot is restricted to wires of so-called *magic radii*, i.e., wires of conductance $G/G_0=1, 3, 6, 12, \dots$, that were shown to be remarkably stable even when allowing symmetry-breaking deformations (Refs. 10 and 30). The lower panel shows the shell potential, and arrows mark the geometries with the longest estimated lifetime (Ref. 32).

The maximum length of freestanding metallic nanowires observed so far in experiments is that of gold wires produced by electron beam irradiation of thin gold films in ultrahigh vacuum,³³ for which lengths of $L \sim 3\text{--}15$ nm are reported. In those experiments, no sign of an onset of the Peierls CDW was seen, presumably indicating that $L < \xi$. However, since the correlation length depends exponentially on the wire radius, *we predict that nanowires of currently available dimensions can be driven into the CDW regime by applying strain.* A tensile force of order of 1 nN can change ξ by orders of magnitude, and thereby drive the system into the CDW regime as soon as the condition (21) is met. Note that since k_F is of order of 1 \AA^{-1} for Na and Au, the thermal length L_T at room temperature is of order of 100 \AA for Na and twice as large for gold, comparable to the lengths of the longest freestanding wires currently produced. By contrast, the elastic mean free path can be several times as long⁴ and electron microscope images of gold nanowires³³ show perfectly regular and disorder-free atomic arrangements. Surface roughness does not play a role in the parameter regime we consider, where electron-shell effects dominate over ionic ordering. Thus, CDW behavior should be observable at room temperature in freestanding metal nanowires under strain, in contrast to the behavior of quasi-one-dimensional organic conductors,³ where CDW behavior is observed only at cryogenic temperatures.

VI. SUMMARY AND DISCUSSION

In conclusion, we have presented a scaling theory of the Peierls CDW in multichannel metal nanowires. Near the critical point, scaling relations for the L , q , and T dependence of the singular part of the free energy, which drives the Peierls instability, were established. A hyperscaling ansatz was verified and the universal scaling function was analyzed, which was found to be logarithmic. The crossover from a regime where the harmonic approximation about a Fermi liquid is valid ($L < L_c$) to that of a fully developed CDW ($L > L_c$) occurs at a critical length of the order of the correlation length ξ_v , which is material dependent. We predict that the Peierls CDW should be observable at room temperature in currently available metal nanowires under an applied strain.

The critical length is shortest in materials whose surface tension is small in natural units (i.e., in units of $E_F k_F^2$). No-

table in this respect²⁹ is Al with $\sigma_s = 0.0018 E_F k_F^2$, some five times smaller than the value for Au. Although Al is a multivalent metal, it has a very free-electron-like band structure in an extended-zone scheme, and thus may be treated within the NFEM, although the continuum approximation is more severe. We thus predict that Al should be an ideal candidate for the observation of the Peierls CDW.

Our findings on the finite-size scaling of the Peierls CDW in metal nanowires are in contrast with previous theoretical studies^{12,13} of mesoscopic rings: For spinless fermions in a one-dimensional ring, the Peierls transition was found to be suppressed for small systems when the number of fermions is odd, but enhanced when the number is even. Obviously, no such parity effect occurs in an open system, such as a metal nanowire suspended between two metal electrodes; we find that the CDW is always suppressed in nanowires with $L \ll \xi_v$. Nonetheless, the correlation length ξ was also found to control the (very different) finite-size scaling in mesoscopic rings.¹³

The finite-size scaling of the Peierls CDW in metal nanowires is similar to that of the metal-insulator transition in the one-dimensional Hubbard model.³⁴ In both cases, there is no phase transition in an infinite system, because the critical electron-phonon coupling and on-site electron-electron repulsion are 0^+ in each case. However, for parameters such that the gap 2Δ in an infinite system is sufficiently small, the system is close to a quantum critical point,^{11,34} and the crossover from Fermi-liquid behavior to a Peierls CDW or Mott insulator, respectively, can be described within hyperscaling theory.

ACKNOWLEDGMENTS

We acknowledge the Aspen Center of Physics, where the final stage of this project was carried out. This work was supported by the DFG and the EU Training Network DI-ENOW (D.F.U. and H.G.) and by NSF Grant No. 0312028 (C.A.S.).

APPENDIX A: LINEAR STABILITY ANALYSIS

This appendix gives details on the linear stability analysis (see Ref. 10) which determines the leading-order change in the grand canonical potential Ω of the electron gas due to a

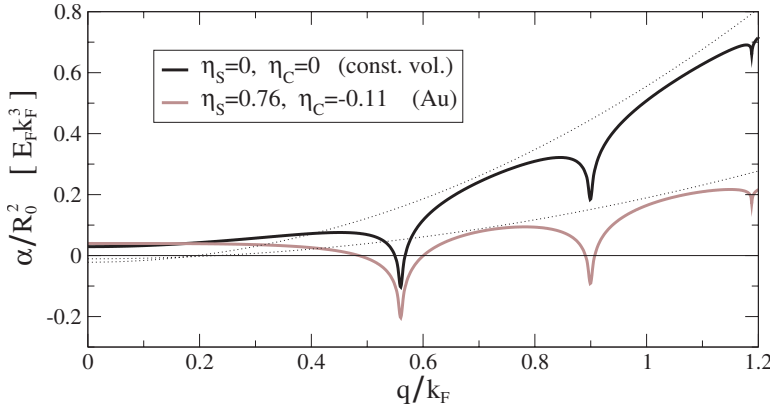


FIG. 5. (Color online) The mode stiffness α computed from Eqs. (A3)–(A5) (solid curves). The dashed curves show the Weyl approximation to α [first two terms on the rhs of Eq. (11)]. The results for gold and for an idealized free-electron metal are shown; in each case, the radius is $R_0 = 5.75k_F^{-1}$ and the length is $L = 1000k_F^{-1}$.

small deformation of a cylindrical nanowire. Since the nanowire is an open system connected to macroscopic metallic electrodes at each end, it is naturally described within a scattering matrix approach. The Schrödinger equation can be expanded as a series in the perturbation, and we solve for the energy-dependent scattering matrix $S(E)$ up to second order. The electronic density of states can then be calculated from

$$D(E) = \frac{1}{2\pi i} \text{Tr} \left\{ S^\dagger(E) \frac{\partial S}{\partial E} - \frac{\partial S^\dagger}{\partial E} S(E) \right\}, \quad (\text{A1})$$

where a factor of 2 for spin degeneracy has been included. Finally, the grand canonical potential Ω is related to the density of states $D(E)$ by

$$\Omega = -k_B T \int dE D(E) \ln[1 + e^{-(E-\mu)/k_B T}], \quad (\text{A2})$$

where k_B is the Boltzmann constant, T is the temperature, and μ is the chemical potential specified by the macroscopic electrodes. We find that the change $\delta\Omega$ due to the deformation of an initially axisymmetric geometry in leading order is quadratic in the Fourier coefficients b_q of the deformation [see Eq. (6)] and can be written as stated in Eq. (9), defining the mode stiffness $\alpha(q, R_0, L, T)$. It is convenient to decompose α into three contributions, $\alpha = \alpha_{\text{diag}} + \alpha_{\text{nond}} + \alpha_{\text{con}}$. The coupling between channels mediated by the surface phonons determines α_{diag} , coming from scattering into the same channel [Eq. (A3)], and α_{nond} , coming from scattering between different channels [Eq. (A4)]:

$$\alpha_{\text{diag}}(q, R_0, L) = \frac{1}{\pi} \sum_n \Theta(E_F - E_n) \left\{ 12E_n k_{F,n} - \frac{4E_n^2}{q} \left[\ln \left| \frac{2k_{F,n} + q}{2k_{F,n} - q} \right| - F((2k_{F,n} + q)L) + F(|2k_{F,n} - q|L) \right] \right\}, \quad (\text{A3})$$

$$\alpha_{\text{nond}}(q, R_0, L) = -\frac{1}{\pi} \sum_{n \neq n'} f_{n,n'} \Theta(E_F - E_n) \left\{ 16k_{F,n} \frac{E_n E_{n'}}{E_n - E_{n'}} + \frac{4E_n E_{n'}}{q} \ln \left| \frac{q^2 + E_{n'} - E_n + 2qk_{F,n}}{q^2 + E_{n'} - E_n - 2qk_{F,n}} \right| + \Theta(E_F - E_{n'}) \frac{4E_n E_{n'}}{q} [F(|q - k_{F,n} - k_{F,n'}|L) - F((q + k_{F,n} + k_{F,n'})L)] \right\}, \quad (\text{A4})$$

$$\alpha_{\text{con}}(q, R_0) = \frac{1}{\pi} \sum_n \Theta(E_F - E_n) 4E_n k_{F,n} \frac{1 + (\eta_c - \eta_s R_0 k_F)(q/k_F)^2}{1 - \eta_s/(R_0 k_F)}. \quad (\text{A5})$$

Here $f_{n,n'} = 1$ for two channels having the same azimuthal symmetry and $f_{n,n'} = 0$ otherwise. The function $F(x) = \text{Ci}(x) - \sin(x)/x$ smoothens the logarithmic divergences so that α_{diag} and α_{nond} are continuous functions having minima of length-dependent depth at $q = 2k_{F,n}$ and $q = k_{F,n} + k_{F,n'}$, respectively. The third contribution [Eq. (A5)] arises due to enforcing the constraint (25) on allowed deformations.

The contribution to Eq. (A4) from evanescent modes with $E_{n'} > E_F$ gives rise to the leading-order q dependence of α_{nond} , which is quadratic. This term therefore essentially captures the change of surface and curvature energy [see Eq. (11)]. Figure 5 compares the mode stiffness α , computed from Eqs. (A3)–(A5), to the Weyl approximation [first two terms on the right-hand side (rhs) of Eq. (11)]. Here, $R_0 = 5.75k_F^{-1}$ and $L = 1000k_F^{-1}$. Both the results for Au ($\eta_s = 0.76$, $\eta_c = -0.11$) and for a pure constant-volume constraint ($\eta_s = \eta_c = 0$) are shown. In both cases, the overall q^2 dependence of α for large q is evident, and consequently, the minimum at $q = 2k_{F,v} \approx 0.56k_F$ is deeper than the other minima.

When examining the softening of phonon modes, the overall increase of $\alpha(q)$ with q allows us to concentrate on the $q_0 \equiv 2k_{F,v}$ mode, where v labels the highest open channel. This mode will always be the dominant one. In general, the

mode stiffness also shows less-pronounced minima at other values $q > q_0$, due to the lower-lying channels, but these contributions are less singular than the q_0 mode. It is therefore possible to approximate α by a smooth contribution $\propto q^2$ plus the explicit terms of Eq. (A3) for the highest open channel.

APPENDIX B: PERTURBATION POTENTIAL MATRIX ELEMENTS

Consider free electrons confined within a cylindrical nanowire of radius R_0 and length L by a step potential $V(r) = V_0 \theta(r - R_0)$, where θ is the step function. The transverse eigenfunctions in polar coordinates are given by $\psi_{mn}^\perp(r, \varphi) = (2\pi)^{-1/2} e^{im\varphi} \chi_{mn}(r)$, where the radial function $\chi_{mn}(r)$ reads

$$\chi_{mn} = N_{mn} \begin{cases} J_m(\sqrt{E_{mn}} r), & r < R_0 \\ \frac{J_m(\sqrt{E_{mn}} R_0) K_m(\sqrt{V_0 - E_{mn}} r)}{K_m(\sqrt{V_0 - E_{mn}} R_0)}, & r > R_0. \end{cases} \quad (\text{B1})$$

Here, N_{mn} is a normalization factor, J_m is the Bessel function of order m , K_m is the modified Bessel function of the second kind of order m , and for simplicity of notation, we use the convention $\hbar^2/2m_e = 1$. The transverse eigenenergies E_{mn} are determined by the continuity of $\partial_r \chi_{mn}/\chi_{mn}$ at $r = R_0$. An axisymmetric perturbation of the wire changes the confinement potential by

$$\delta V(r, z) = V_0 [\theta(r - R_0 - \delta R(z)) - \theta(r - R_0)], \quad (\text{B2})$$

where the variation in radius is given by $\delta R(z)/R_0 = \sum_q b_q e^{iqz}$ and the perturbation wave vectors q are restricted to integer multiples of $2\pi/L$. We expand the matrix elements of δV with respect to the unperturbed eigenfunctions $\Psi_{mnk}(r, \varphi, z) = L^{-1/2} e^{ikL} \psi_{mn}^\perp(r, \varphi)$ to first order in b_q and get

$$\langle mnk | \delta V | \bar{m} \bar{n} \bar{k} \rangle \simeq -\delta_{m\bar{m}} V_0 R_0 \chi_{mn}(R_0) \chi_{\bar{m}\bar{n}}(R_0) \times \sum_q b_q \frac{1 - e^{i(\bar{k} - k + q)L}}{i(\bar{k} - k + q)L}. \quad (\text{B3})$$

Taking the limit $V_0 \rightarrow \infty$, we get

$$\lim_{V_0 \rightarrow \infty} \langle mnk | \delta V | \bar{m} \bar{n} \bar{k} \rangle \simeq 2\sqrt{E_{mn} E_{\bar{m}\bar{n}}} \sum_q b_q \frac{1 - e^{i(\bar{k} - k + q)L}}{i(\bar{k} - k + q)L}. \quad (\text{B4})$$

In the limit of $L \rightarrow \infty$, we have

$$\lim_{\substack{V_0 \rightarrow \infty \\ L \rightarrow \infty}} \langle mnk | \delta V | \bar{m} \bar{n} \bar{k} \rangle \simeq -2\sqrt{E_{mn} E_{\bar{m}\bar{n}}} b_q \delta_{\bar{k}, k+q} \quad (\text{B5})$$

and recover a coupling of states with $\bar{k} = k + q$, only.

¹H. Fröhlich, Proc. R. Soc. London, Ser. A **223**, 296 (1954).

²R. E. Peierls, *Quantum Theory of Solids* (Oxford University Press, London, 1956).

³G. Grüner, Rev. Mod. Phys. **60**, 1129 (1988).

⁴N. Agraït, A. Levy Yeyati, and J. M. van Ruitenbeek, Phys. Rep. **377**, 81 (2003).

⁵H. W. Yeom, S. Takeda, E. Rotenberg, I. Matsuda, K. Horikoshi, J. Schaefer, C. M. Lee, S. D. Kevan, T. Ohta, T. Nagao, and S. Hasegawa, Phys. Rev. Lett. **82**, 4898 (1999).

⁶J. R. Ahn, H. W. Yeom, H. S. Yoon, and I.-W. Lyo, Phys. Rev. Lett. **91**, 196403 (2003).

⁷J. R. Ahn, J. H. Byun, H. Koh, E. Rotenberg, S. D. Kevan, and H. W. Yeom, Phys. Rev. Lett. **93**, 106401 (2004).

⁸J. R. Ahn, P. G. Kang, K. D. Ryang, and H. W. Yeom, Phys. Rev. Lett. **95**, 196402 (2005).

⁹P. C. Snijders, S. Rogge, and H. H. Weitering, Phys. Rev. Lett. **96**, 076801 (2006).

¹⁰D. F. Urban and H. Grabert, Phys. Rev. Lett. **91**, 256803 (2003).

¹¹J. A. Hertz, Phys. Rev. B **14**, 1165 (1976).

¹²B. Nathanson, O. Entin-Wohlman, and B. Mühlischlegel, Phys. Rev. B **45**, 3499 (1992).

¹³G. Montambaux, Eur. Phys. J. B **1**, 377 (1998).

¹⁴C.-H. Zhang, F. Kassubek, and C. A. Stafford, Phys. Rev. B **68**, 165414 (2003).

¹⁵K. A. Matveev and L. I. Glazman, Phys. Rev. Lett. **70**, 990 (1993).

¹⁶F. Kassubek, C. A. Stafford, and H. Grabert, Phys. Rev. B **59**, 7560 (1999).

¹⁷C.-H. Zhang, J. Bürki, and C. A. Stafford, Phys. Rev. B **71**, 235404 (2005).

¹⁸In that respect, the situation is considerably different from, e. g., quasi-one-dimensional organic conductors where interactions lead to important qualitative effects.

¹⁹C. A. Stafford, D. Baeriswyl, and J. Bürki, Phys. Rev. Lett. **79**, 2863 (1997).

²⁰J. Bürki and C. A. Stafford, Appl. Phys. A: Mater. Sci. Process. **81**, 1519 (2005).

²¹The modified Bessel functions (of the first kind) $I_n(x)$ are solutions of the differential equation $x^2 y'' + xy' - (x^2 + n^2)y = 0$ that are regular at $x = 0$.

²²Note that the mode stiffness $\alpha(q, R_0, L, T)$ appearing in Eq. (9) essentially determines the stability of the nanowire: if α is positive for all values of the perturbation wave vector q , all small deformations of the cylindrical geometry lead to an increase of Ω and are therefore suppressed.

²³The cosine integral function is defined as $\text{Ci}(x) = -\int_x^\infty dt \cos(t)/t$.

²⁴Hereby, we need to remember that $E_{\text{sing}}/L = \alpha |b_{2k_{F,v}}|^2$ and $\Delta_v^2 = 4E_v^2 |b_{2k_{F,v}}|^2$.

²⁵This expression can be derived by using $R_0 b_q(t) = \sqrt{\hbar/2m\omega L} (\hat{a}_q e^{-i\omega t} + \hat{a}_{-q}^\dagger e^{i\omega t})$, which relates the deformation amplitude to the phonon operators, and by assuming thermal occupation numbers. Furthermore, we have approximated the sum over q by an integral.

²⁶The modified Bessel functions of the second kind $K_n(x)$ satisfy the differential equation $x^2 y'' + xy' - (x^2 + n^2)y = 0$, with $K_n(x)$ having a singularity at $x = 0$ and tending to zero as $x \rightarrow \infty$.

²⁷M. Abramowitz and I. E. Stegun, *Handbook of Mathematical Functions* (Dover, New York, 1974).

²⁸D. F. Urban, J. Bürki, C. A. Stafford, and H. Grabert, Phys. Rev. B **74**, 245414 (2006).

²⁹W. R. Tyson and W. A. Miller, Surf. Sci. **62**, 267 (1977).

³⁰D. F. Urban, J. Bürki, C. H. Zhang, C. A. Stafford, and H. Grabert, Phys. Rev. Lett. **93**, 186403 (2004).

³¹For completeness, the whole sequence of magic radii is included in Fig. 4 although it is clear that the continuum model used for our calculations is at its limits of validity for a wire of

conductance $1G_0$.

³²J. Bürki, C. A. Stafford, and D. L. Stein, Phys. Rev. Lett. **95**, 090601 (2005).

³³Y. Kondo and K. Takayanagi, Science **289**, 606 (2000).

³⁴C. A. Stafford and A. J. Millis, Phys. Rev. B **48**, 1409 (1993).